Journal of Zhejiang University-SCIENCE A (Applied Physics & Engineering)
www.jzus.zju.edu.cn; www.springer.com/journal/11582
E-mail: jzus_a@zju.edu.cn

Electronic Supplementary Materials

For https://doi.org/10.1631/jzus.A2300361

Effects of high geotemperature and high altitude on the pressure wave of high-speed trains running in a long tunnel

Lei LIU, Lin JING✉, Tian LI, Kaiyun WANG

State Key Laboratory of Rail Transit Vehicle System, Southwest Jiaotong University, Chengdu 610031, China

✉ Lin JING, jinglin@swjtu.edu.cn

S1 Introduction

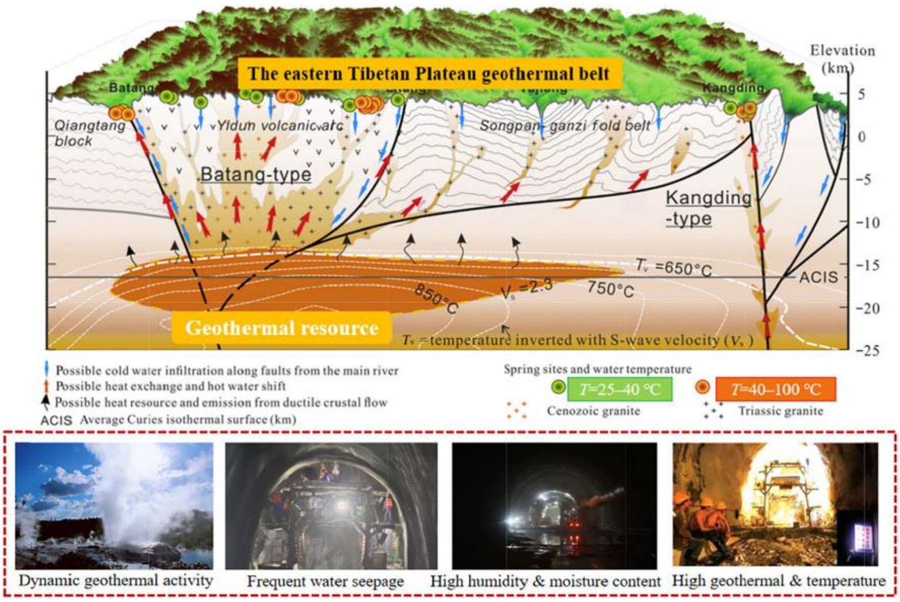

Fig. S1 Geological condition of the tunnel construction (Zhao et al., 2023)

S2 Numerical simulation and algorithm verification

Table S1 Grid parameters for three schemes

Scheme	Minimum size (m)		Total number (million)
	Train surface	Tunnel wall	
Coarse	0.1	0.5	5.5
Middle	0.05	0.2	7.7
Fine	0.02	0.1	19.8

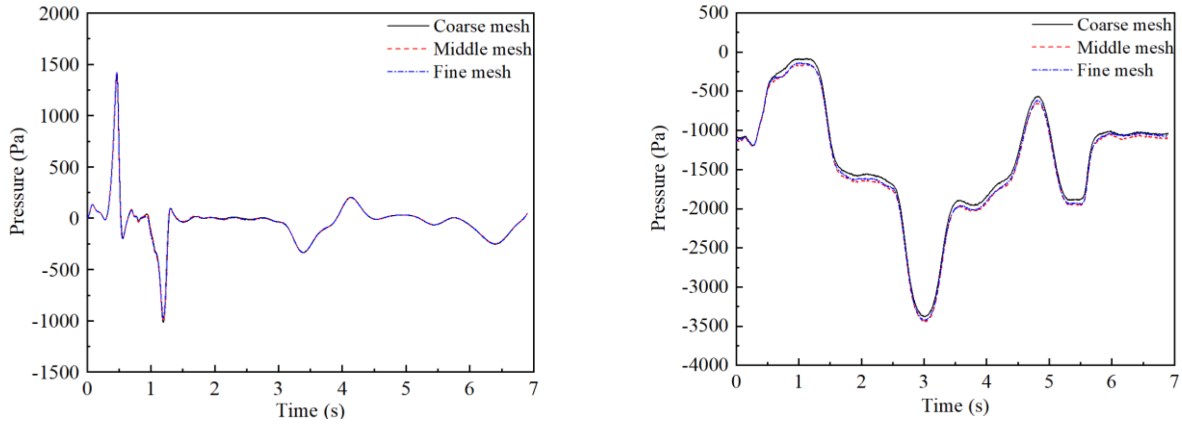

(a) (b)

Fig. S2 Comparison of pressure variation curves of observation points calculated using different grid schemes: (a) on the tunnel wall; (b) on the train surface

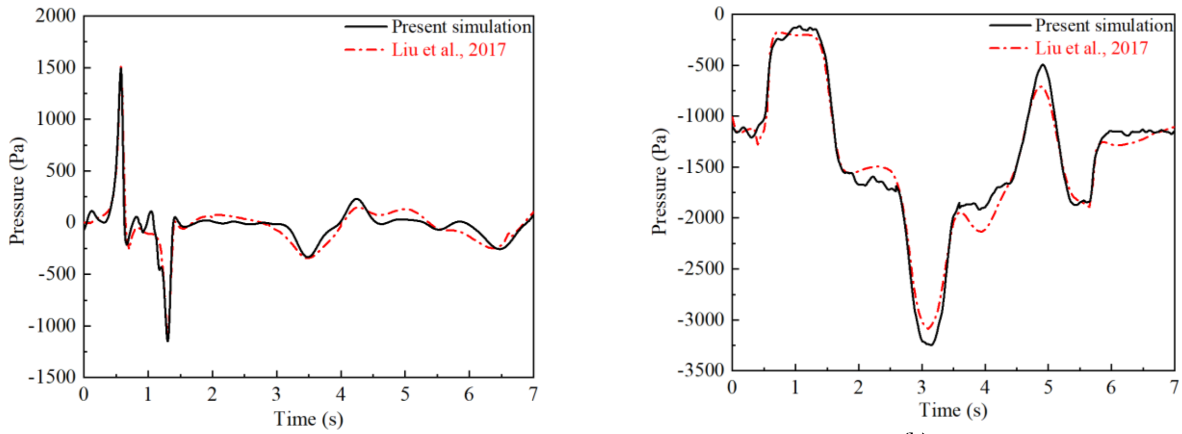

(a) (b)

Fig. S3 Comparison of the observation point pressure when trains pass through tunnels: (a) on the tunnel wall; (b) on the train surface

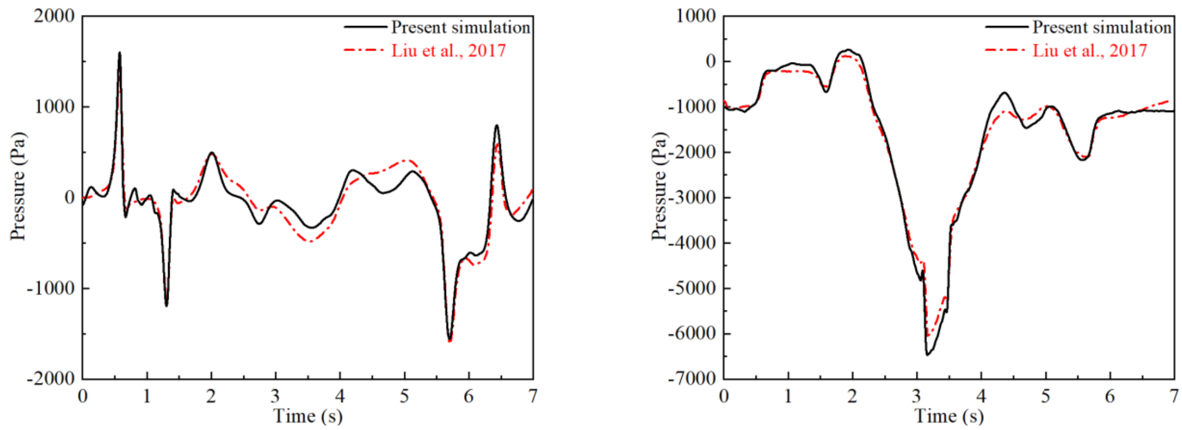

(a) (b)

Fig. S4 Comparison of the observation point pressure when two trains pass by each other in a tunnel: (a) on the tunnel wall; (b) on the train surface.

S3 Determination of the computational tunnel length

S3.1 Computational tunnel length for the train passing through the tunnel

S3.1.1 Pressure wave characteristics in the tunnel

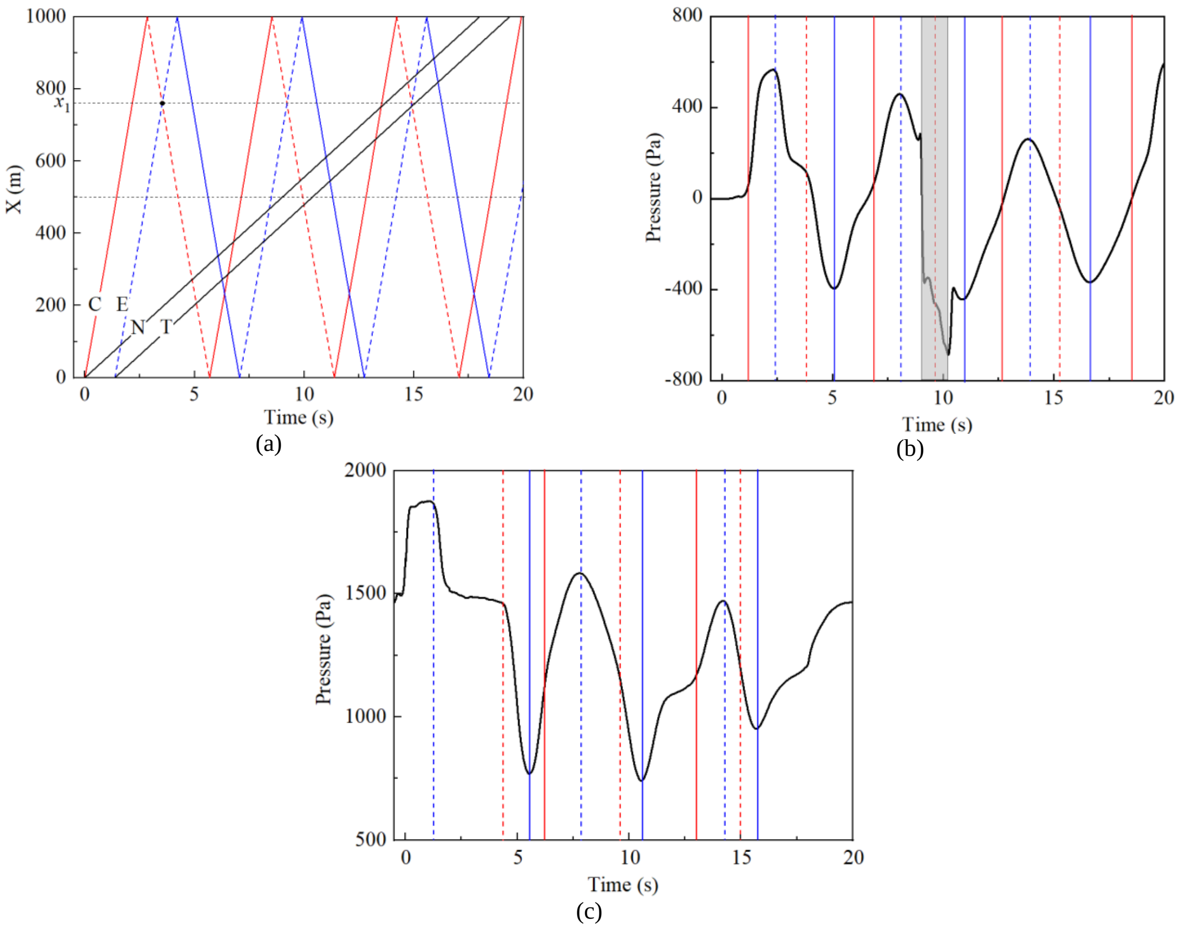

Fig. S5 Propagation processes of pressure waves and pressure variation curves of observation points when trains pass through tunnels: (a) propagation processes of pressure waves. The C, E, N, T denote the compression wave, expansion wave, the tip of the train nose and tail respectively, and the x_1 denotes the position where the expansion wave reflected by the initial compression wave encounters the initial expansion wave for the first time; (b) tunnel midpoint (TU_25). The grey area denotes the process of the train-passage; (c) train nose tip (TR_1)

S3.1.2 Determination of tunnel length

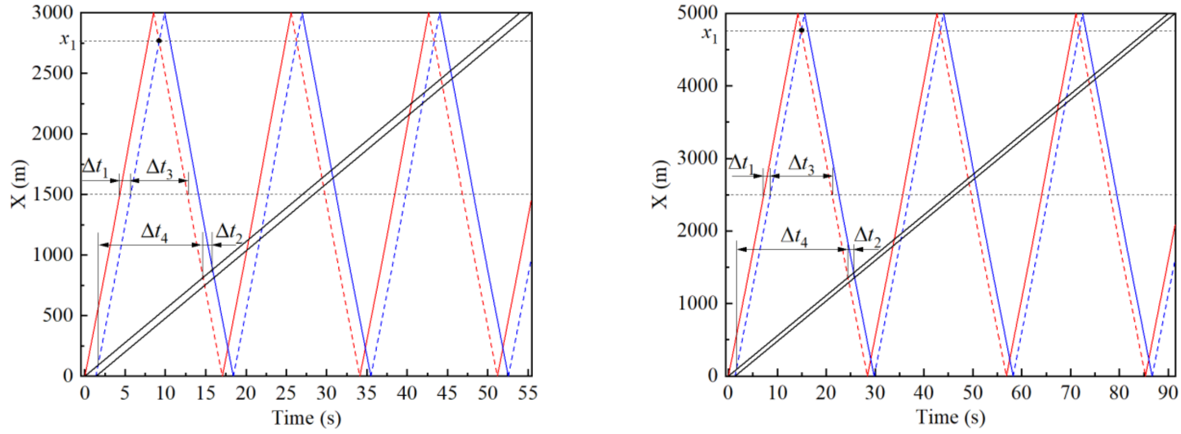

(a) (b)

Fig. S6 Propagation processes of the pressure waves when trains pass through the 3 km and 5 km tunnels: (a) in the 3 km tunnel; (b) in the 5 km tunnel

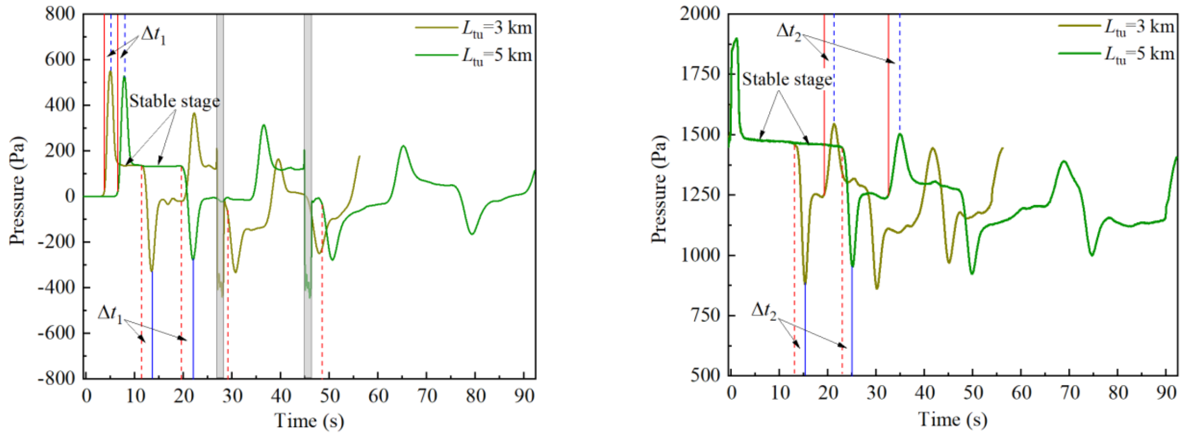

(a) (b)

Fig. S7 Pressure variation curves of observation points when trains pass through the 3 km and 5 km tunnels: (a) tunnel midpoint (TU_25); (b) tip of the train nose (TR_1)

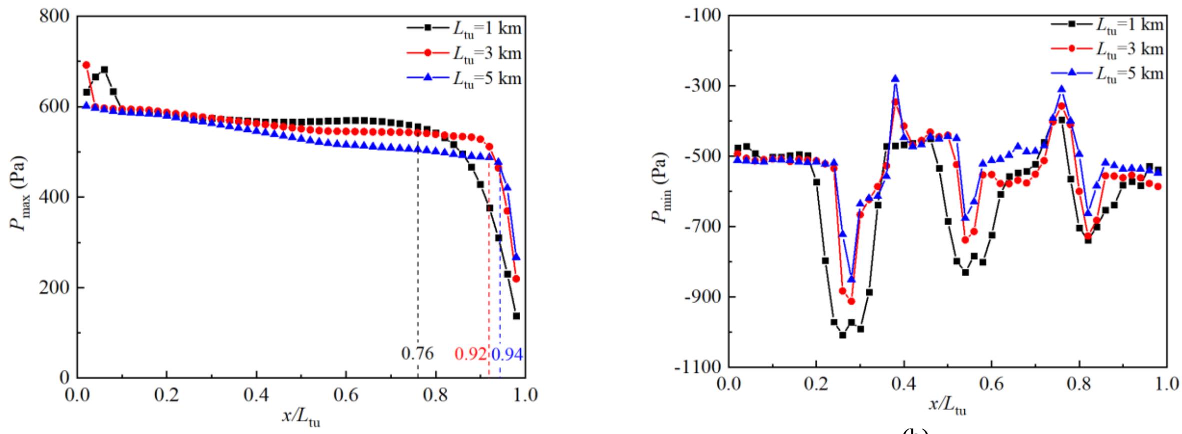

(a) (b)

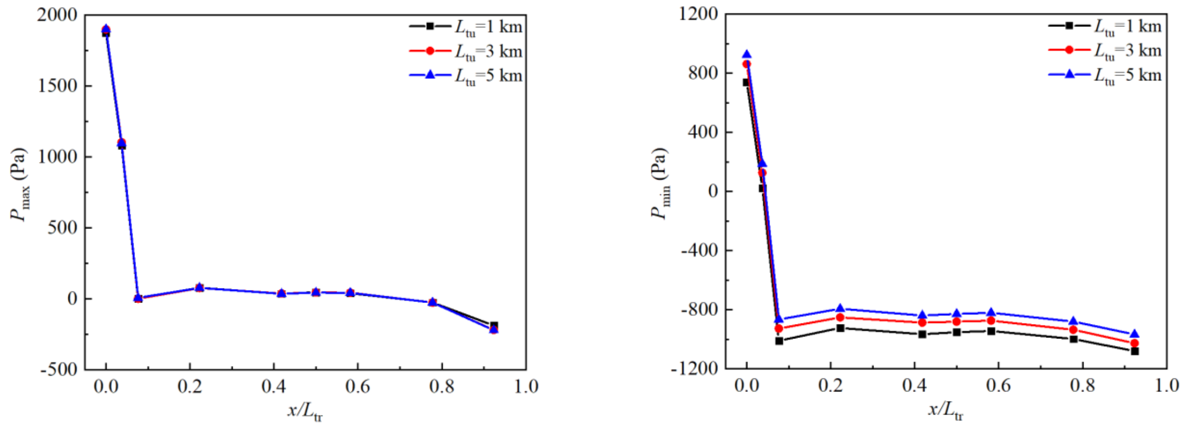

(c) (d)

Fig. S8 Distributions of P_{max} and P_{min} along the tunnel and train when trains pass through tunnels of different lengths: (a), (b) P_{max} and P_{min} along the tunnel; (c), (d) P_{max} and P_{min} along the train

S3.2 Computational tunnel length for two trains passing by each other in a tunnel

S3.2.1 Pressure wave characteristics in the tunnel

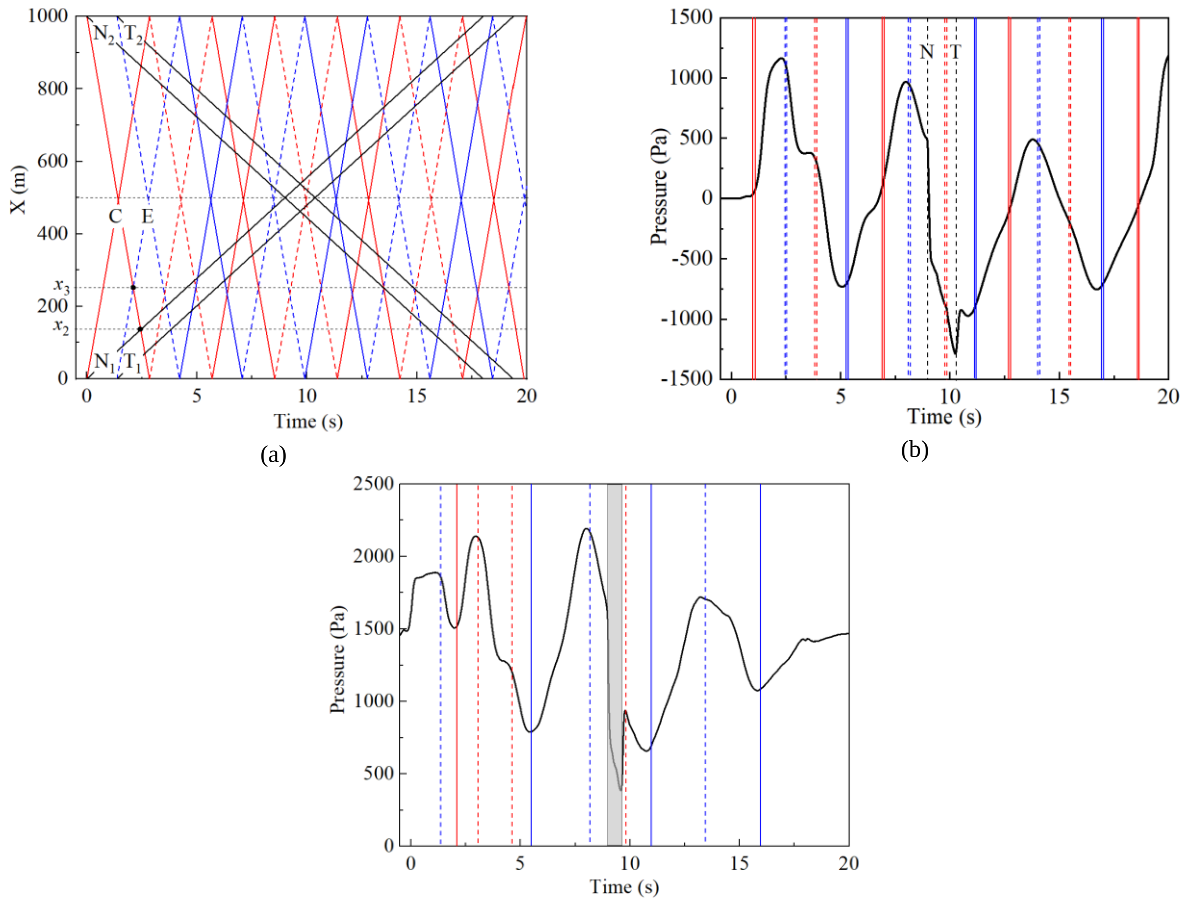

(a) (b) (c)

Fig. S9 Propagation processes of pressure waves and pressure variation curves of observation points when two trains pass by each other in a tunnel: (a) Propagation processes of pressure waves. The x_2 and x_3 respectively denote the position where the nose tip of the train 1 encounters the compression wave for the first time, and compression waves and expansion waves on the same side of the tunnel midpoint encounter for the first time; (b) TU_25; (c) TR_1

S3.2.2 Determination of tunnel length

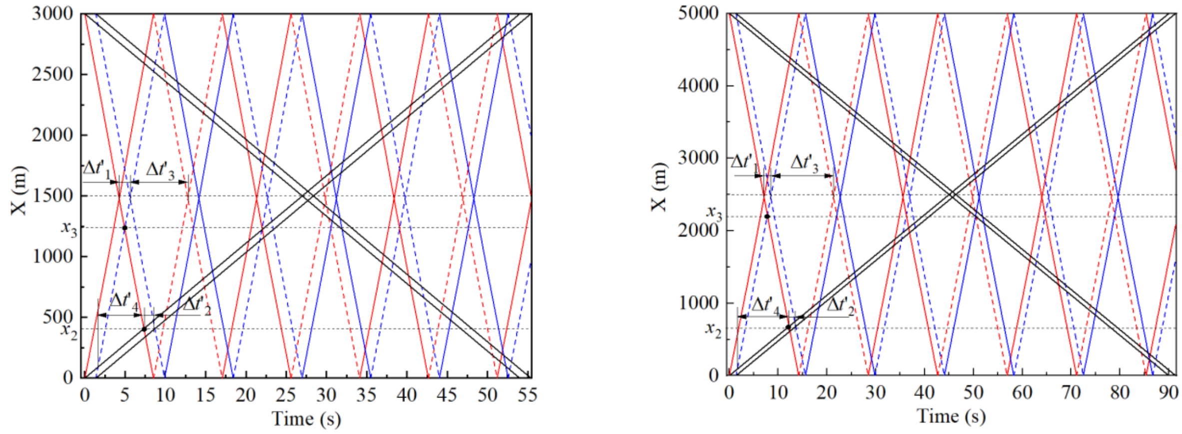

(a) (b)

Fig. S10 Propagation processes of the pressure waves when two trains pass by each other in the 3 km and 5 km tunnels: (a) in 3 km tunnel; (b) in 5 km tunnel

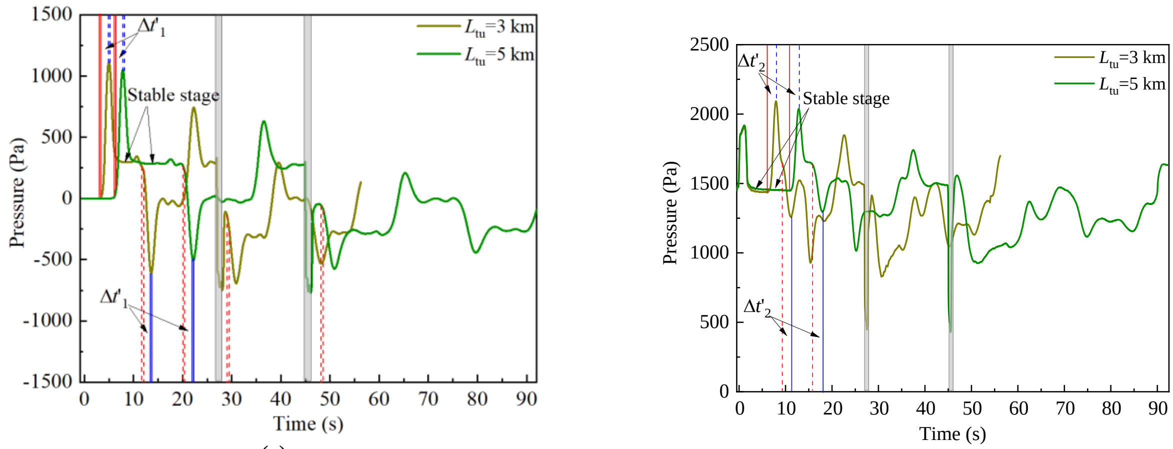

(a)

(b)

Fig. S11 Pressure variation curves of observation points when two trains pass by each other in the 3 km and 5 km tunnels: (a) TU_25; (b) TR_1

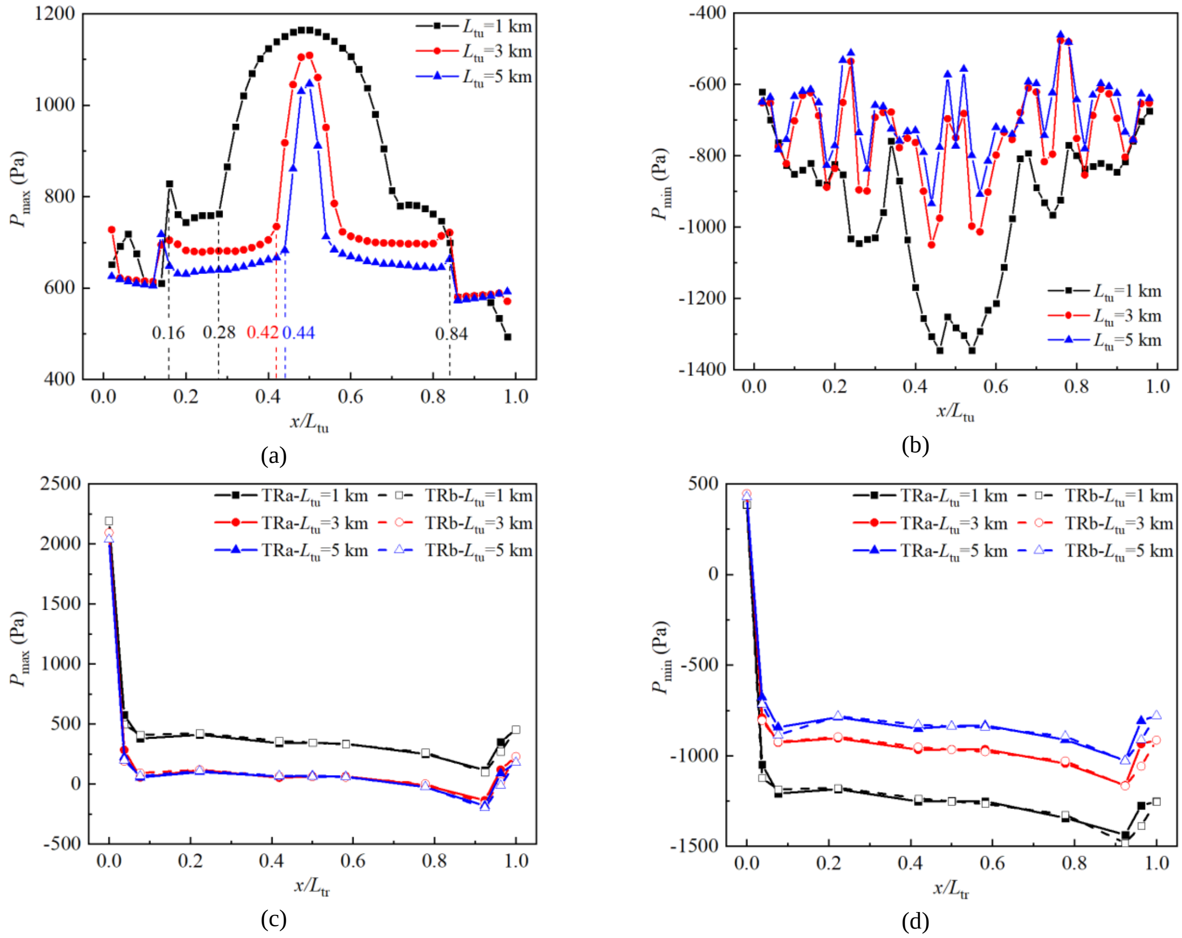

Fig. S12 Distributions of P_{max} and P_{min} along the tunnel and train when two trains pass by each other in tunnels of different lengths: (a), (b) P_{max} and P_{min} along the tunnel; (c), (d) P_{max} and P_{min} along the train. TRa and TRb denote the measuring points on the train surface close to the tunnel wall and close to the tunnel centerline respectively

S4 Simulation results and discussion

S4.1 Effect of high geotemperature on the pressure wave

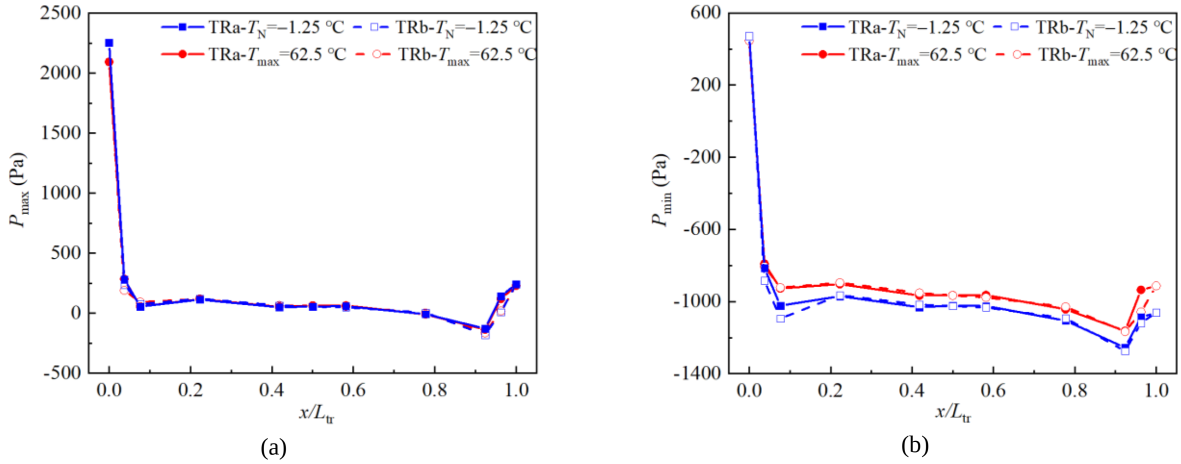

Fig. S13 Distributions of P_{max} and P_{min} along the train when two trains pass by each other in the ambient-temperature tunnel and high-temperature tunnel: (a) P_{max}; (b) P_{min}

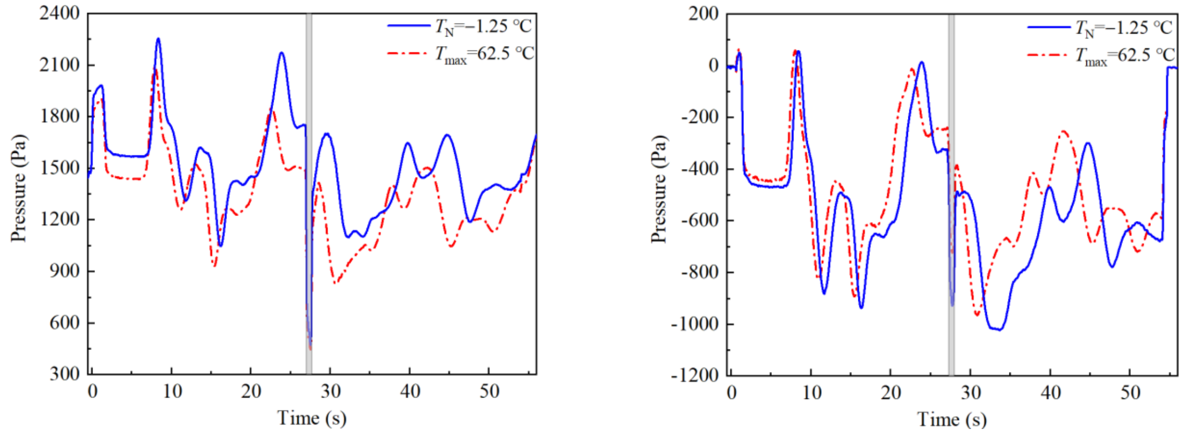

(a) (b)

Fig. S14 Pressure variation curves of observation points on the train when two trains pass by each other in the ambient-temperature tunnel and high-temperature tunnel: (a) TR_1; (b) TR_3b

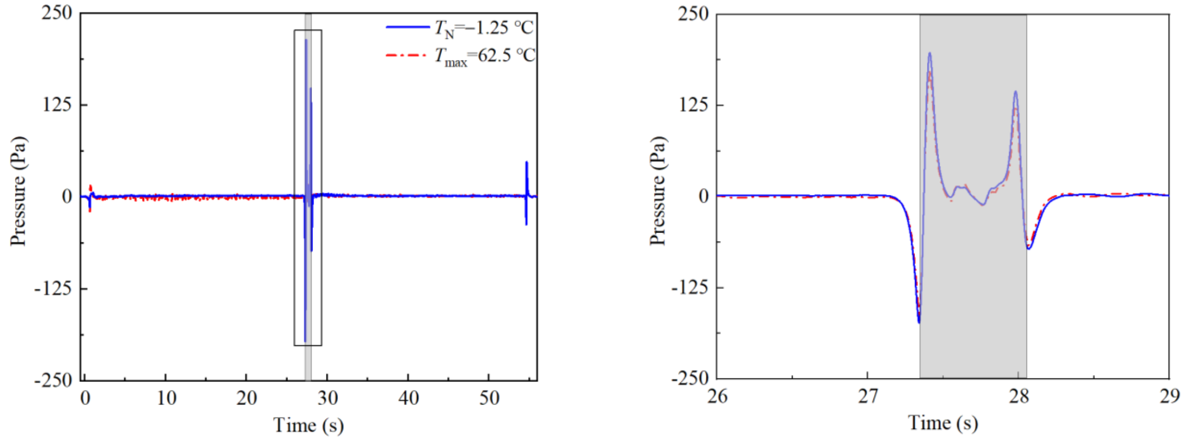

(a) (b)

Fig. S15 Variation curve of the pressure difference between observation points TR_6a and TR_6b when two trains pass by each other in the ambient-temperature tunnel and high-temperature tunnel. The right part is the enlargement of the middle rectangle in the left part

S4.2 Effect of high altitude on pressure wave

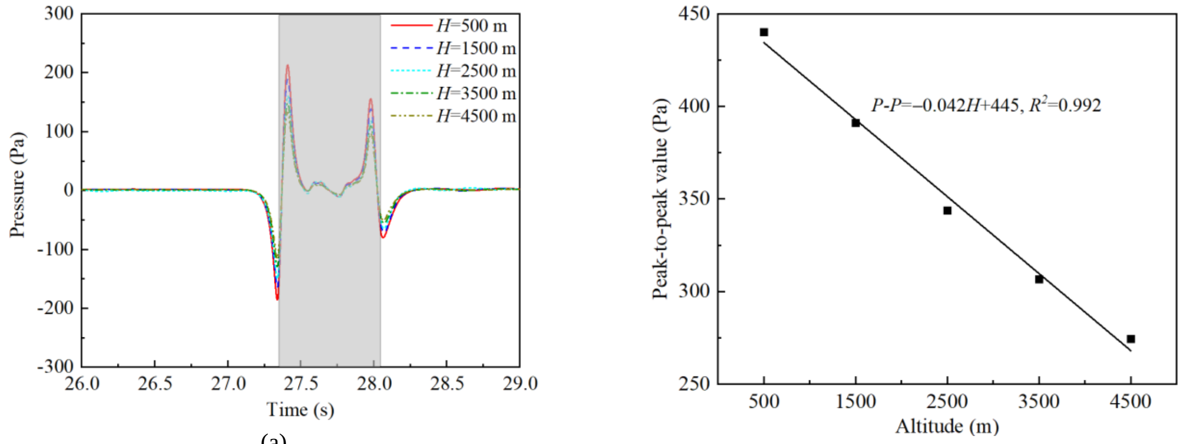

(a) (b)

Fig. S16 The pressure difference between observation points TR_6a and TR_6b during intersecting in the high-temperature tunnels of different altitudes: (a) variation curve; (b) fitting curve between the peak-peak value and the altitude

References

Zhao KM, Yuan YP, Jiang FJ, et al., 2023. Numerical investigation on temperature–humidity field under mechanical ventilation in the construction period of hot-humid tunnel along the Sichuan–Tibet Railway. *Underground Space*, 8:123-143. https://doi.org/10.1016/j.undsp.2022.04.004

Liu TH, Chen ZW, Chen XD, et al., 2017b. Transient loads and their influence on the dynamic responses of trains in a tunnel. *Tunnelling and Underground Space Technology*, 66:121-133. https://doi.org/10.1016/j.tust.2017.04.009